Iterative Reconstruction Based on Median Root Prior in Quantification of Myocardial Blood Flow and Oxygen Metabolism

Chietsugu Katoh, Ulla Ruotsalainen, Hanna Laine, Sakari Alenius, Hidehiro Iida , Pirjo Nuutila and Juhani Knuuti

Turku PET Centre, Turku; Signal Processing Laboratory, Tampere University of Technology, Tampere, Finland; Department of Nuclear Medicine, Hokkaido University School of Medicine, Sapporo; Research Institute for Brain and Blood Vessels, Akita, Japan

The aim of this study was to compare reproducibility and accuracy of two reconstruction methods in quantification of myocardial blood flow and oxygen metabolism with ^{15}O-labeled tracers and PET. A new iterative Bayesian reconstruction method based on median root prior (MRP) was compared with filtered backprojection (FBP) reconstruction method, which is traditionally used for image reconstruction in PET studies. **Methods:** Regional myocardial blood flow (rMBF), oxygen extraction fraction (rOEF) and myocardial metabolic rate of oxygen consumption ($rMMRO_2$) were quantified from images reconstructed in 27 subjects using both MRP and FBP methods. For each subject, regions of interest (ROIs) were drawn on the lateral, anterior and septal regions on four planes. To test reproducibility, the ROI drawing procedure was repeated. By using two sets of ROIs, variability was evaluated from images reconstructed with the MRP and the FBP methods. **Results:** Correlation coefficients of mean values of rMBF, rOEF and $rMMRO_2$ were significantly higher in the images reconstructed with the MRP reconstruction method compared with the images reconstructed with the FBP method (rMBF: MRP $r = 0.896$ versus FBP $r = 0.737$, $P < 0.001$; rOEF: 0.915 versus 0.855, $P < 0.001$; $rMMRO_2$: 0.954 versus 0.885, $P < 0.001$). Coefficient of variation for each parameter was significantly lower in MRP images than in FBP images (rMBF: MRP 23.5% ± 11.3% versus FBP 30.1% ± 14.7%, $P < 0.001$; rOEF: 21.0% ± 11.1% versus 32.1% ± 19.8%, $P < 0.001$; $rMMRO_2$: 23.1% ± 13.2% versus 30.3% ± 19.1%, $P < 0.001$). **Conclusion:** The MRP reconstruction method provides higher reproducibility and lower variability in the quantitative myocardial parameters when compared with the FBP method. This study shows that the new MRP reconstruction method improves accuracy and stability of clinical quantification of myocardial blood flow and oxygen metabolism with ^{15}O and PET.

Key Words: PET; ^{15}O; iterative reconstruction; myocardial blood flow; myocardial oxygen metabolism

J Nucl Med 1999; 40:862–867

The filtered backprojection (FBP) method is a standard procedure for reconstruction of PET images from acquired radiation profiles. However, artifacts resulting from the FBP method cause limited image quality in studies with low counts or when hot areas are present in the field of view (*1*). Recently, iterative image reconstruction algorithms, such as maximum likelihood expectation maximization (MLEM), have been applied to PET data. Iterative reconstruction algorithms are more accurate as a statistical model for the data. This enables better noise reduction and, thus, leads to a better image quality than the FBP method (*2–4*). Clinical advantages of the MLEM method have been reported in oncologic studies (*1,5*). However, the MLEM image quality is very sensitive to the number of iterations, because a large number of iterations leads to images with checkerboard noise (*6*). On the other hand, a limited number of iterations results in biased images that may lead to errors in quantitative PET measurements.

We have introduced a new iterative reconstruction algorithm, which uses median root prior (MRP) for emission PET data (*7*). It has been shown to be insensitive to the number of iterations and to any organ specific reconstruction parameters. The use of median filtering in the reconstruction process allows both noise reduction and edge preservation and, thus, leads to improved image quality.

To assess the clinical usefulness of the MRP method, we applied it to quantitative myocardial PET studies performed with ^{15}O-labeled tracers. The theory and application of noninvasive quantification of regional myocardial blood flow (rMBF) and oxygen metabolism with ^{15}O-labeled tracers and PET has been introduced recently (*8*). In this study, this model was applied to quantitate rMBF, oxygen extraction fraction (rOEF) and myocardial metabolic rate of oxygen consumption ($rMMRO_2$) in images reconstructed with both the MRP and the FBP methods. Quantification of rOEF and $rMMRO_2$ was assumed to benefit most from the new reconstruction method, because the ^{15}O images were noisy as a result of a short acquisition time.

In this study, reproducibility and accuracy of a new iterative Bayesian reconstruction method, based on MBP, was compared with the FBP reconstruction method. In addition, variability in the average and regional metabolic

Received Apr. 3, 1998; revision accepted Jul. 8, 1998.

For correspondence or reprints contact: Chietsugu Katoh, MD, Department of Nuclear Medicine, Hokkaido University School of Medicine, N-15, W-7, Kita-ku, Sapporo, 060–8638 Japan.

parameters calculated from images reconstructed with the MRP and the FBP methods was compared.

MATERIALS AND METHODS

Subjects

PET studies were performed under standardized metabolic conditions for 27 men. The study group consisted of 11 healthy subjects (age 40.6 ± 3.9 y, body mass index 25.3 ± 2.7 kg/m^2) and 16 subjects with essential hypertension (age 41.3 ± 4.0 y, body mass index 26.6 ± 1.6 kg/m^2). All subjects had normal urine analysis, blood counts, electrolytes, glycosylated hemoglobin concentration, renal and liver function tests and no symptoms or signs of ischemia in exercise echocardiography. The nature, purpose and potential risks of the study were explained to all subjects before they gave their written consent to participate. The study was approved by the Ethics Committee of the Turku University Central Hospital.

Production of [^{15}O]CO, [^{15}O]H_2O and [^{15}O]O_2

For production of ^{15}O compounds, a low-energy deuteron accelerator was used (Cyclone 3; Ion Beam Application Inc., Louvain-la-Neuve, Belgium). [^{15}O]H_2O was produced with a dialysis technique in a continuously working water module. Sterility and pyrogen tests were performed daily to verify the purity of the product. ^{15}O oxygen was processed to [^{15}O]CO in a charcoal oven at 950°C. Gas chromatographic analysis was performed to verify the purity of the product before each study.

Data Acquisition

PET studies were performed with an ECAT 931/08–12 scanner (Siemens/CTI Corp., Knoxville, TN), which produces 15 slices in a 10.5-cm axial field of view. All subjects fasted overnight before the PET scanning. The subjects were positioned supine in the tomograph. Before emission scans, a transmission scan was performed for 20 min with a removable ^{68}Ge ring source.

Blood Volume Image. The blood volume images were produced in the following way. The subject's nostrils were closed and the subject inhaled [^{15}O]CO for 2 min (0.1 4% CO mixed with room air). After the inhalation of the tracer, 2 min were allowed for the CO to combine with hemoglobin, before a static scan of 4 min was started. During the 4-min scan period, venous blood samples were drawn every 2 min and the radioactivity concentration in the whole blood was measured with an automatic gamma counter (Wizard 1480; Wallac Inc., Turku, Finland). The inhaled total dose in the [^{15}O]CO examination was 3240 ± 320 MBq.

Blood Flow Image. ^{15}O radioactivity had returned to the background levels 10–15 min after the blood volume scan and [^{15}O]H_2O was infused into an antecubital vein as a slow (2 min) infusion. The total administered dose of [^{15}O]H_2O was 1610 ± 150 MBq. A 20-frame dynamic PET scan was performed for 6 min consisting of 6 × 5-s, 6 × 15-s and 8 × 30-s frames.

O_2 Steady State Image. Approximately 15 min after the [^{15}O]H_2O scan, a continuous inhalation of [^{15}O]O_2 (2.5 MBq/mL at a flow rate of 500 mL/min) was started. A PET scan was performed simultaneously for 16 min. The total inhaled dose of [^{15}O]O_2 was 3650 ± 560 MBq. After an 8-min inhalation, a steady state concentration of [^{15}O]O_2 was established in the heart, and an image was acquired for 8 min.

Reconstruction Methods

All emission images were reconstructed with the MRP and the FBP methods. The spatial resolutions in the MRP and FBP images were measured by using a line source of 6 mm inner diameter, placed in the center of the field of view perpendicular to the image plane. The in-plane resolution was 8 mm full width at half maximum (FWHM) in a 128 × 128 matrix image reconstructed using the MRP method, with weight of the prior 0.3 and number of iterations 150. The theory of the MRP reconstruction method has been documented elsewhere (*7*). The in-plane resolution was 9.5 mm FWHM in images reconstructed into a 128 × 128 matrix using the FBP method with a Hann filter (cutoff frequency 0.5). All data were corrected for dead-time, decay and measured photon attenuation.

Data Processing

The analysis of PET images was accomplished with an image analysis package (Dr. View; Asahi-Kasei, Tokyo, Japan) and special dedicated software. For calculation of rMBF, rOEF and $rMMRO_2$, images were processed according to the standard procedure (*8*). The procedure to derive the rMBF has been developed to correct for the systematic underestimation in measurements of myocardial radiotracer concentration as a result of wall motion and transmural wall thickness in PET myocardial blood flow studies with [^{15}O]H_2O (*9*). Blood volume images were calculated by dividing the [^{15}O]CO images by the mean blood radioactivity concentration (measured with an automatic gamma counter). [^{15}O]H_2O washout images were calculated by first integrating the [^{15}O]H_2O dynamic images over the washout period and then subtracting the scaled blood volume images from these (*9*). The extravascular density images, which were used for drawing the myocardial regions of interest (ROIs), were calculated by subtracting the blood volume image from the corresponding transmission image normalized to the density of blood. These images identify extravascular myocardial tissue mass and allow accurate localization of the myocardial walls (*9*).

Region of Interest Definition

Myocardial ROIs were drawn manually in the lateral, anterior and septal walls in four midventricular slices of the extravascular density images; thus, 12 myocardial ROIs were positioned in one process (Fig. 1). The slices near the diaphragm and the apical

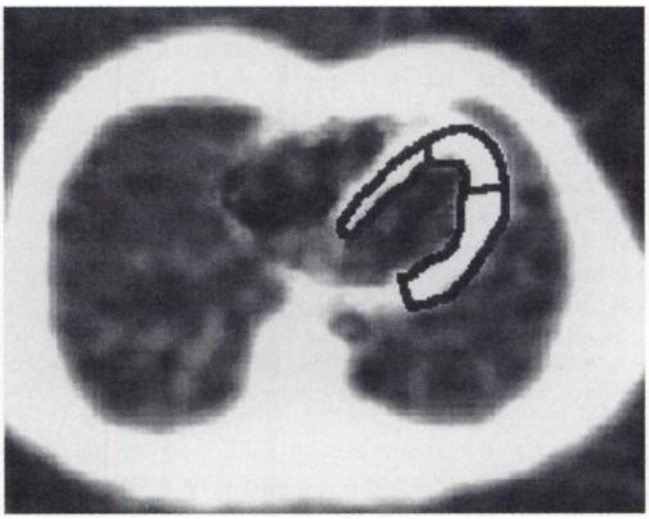

FIGURE 1. Positioning of ROIs on lateral, anterior and septal regions on left ventricular wall. Myocardial ROIs were drawn manually on four midventricular slices of extravascular density images, and data were analyzed independently for each slice.

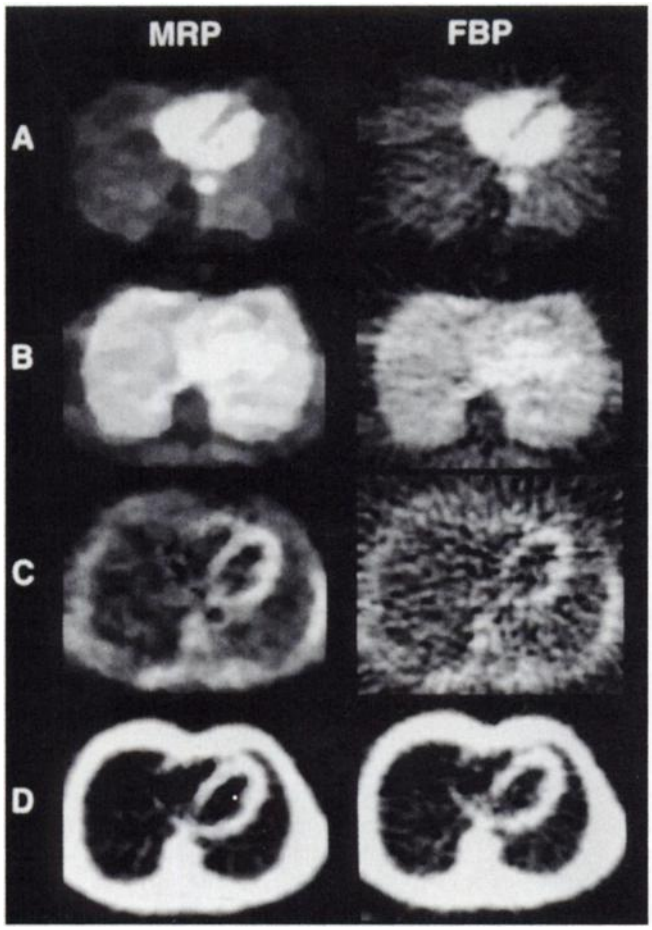

FIGURE 2. Images reconstructed with MRP (left side) and FBP methods (right side). Blood volume images derived from [^{15}O]CO scan (A), [^{15}O]O_2 steady state images (B), [^{15}O]H_2O washout phase images (C) and extravascular density images (D).

region were avoided. The septal ROI was slightly shifted to the left ventricular side (*10*). A large and a small ROI were drawn in the left ventricular chamber for definition of input function (*11*). A pulmonary ROI was positioned in the peripheral lung area (*8*).

Four sets of ROIs were drawn for each subject by one operator. The following four processes were performed:

1. MRP-1: A set of ROIs was positioned on the extravascular density images, derived from the MRP images, and the metabolic parameters were calculated with the MRP images.
2. MRP-2: One week after the MRP-1 process, another set of the ROIs was redrawn without referring to the previous one on the MRP extravascular density images, and the metabolic parameters were calculated with the MRP images.
3. FBP-1: Several months after the MRP-2 process, a set of ROIs was positioned on the FBP extravascular density images, and the metabolic parameters were calculated with the FBP images.
4. FBP-2: One week after the FBP-1 process, another set of the ROIs was redrawn without referring to the previous one on the FBP extravascular density images, and the metabolic parameters were calculated with the FBP images.

The arterial and myocardial tissue time-activity curves were generated from the dynamic [^{15}O]H_2O data. The rMBF was calculated with these time-activity curves, according to the previously described nonlinear least square fitting method (*9,11,12*). The rOEF was derived with the [^{15}O]O_2 steady state method, and $rMMRO_2$ was calculated as a product of rMBF, rOEF and oxygen content in arterial blood (*8*).

Statistical Analysis

To evaluate the reproducibility of the results, Pearson's correlation coefficients were calculated for rMBF, rOEF and $rMMRO_2$ derived from MRP images (MRP-1 versus MRP-2) and FBP images (FBP-1 versus FBP-2). The differences in these correlation coefficients were compared using Fisher z-transformation.

Differences in rMBF, rOEF and $rMMRO_2$ values between MRP-1 and FBP-1 of each subject were examined with paired Student *t* test. Therefore, the calculated differences in rMBF, rOEF and $rMMRO_2$ included only variability between the reconstruction methods and not variability between subjects.

To estimate the regional variability of each subject, the coefficients of variations of each parameter over four transaxial slices in the MRP images (MRP-1 and MRP-2) and in the FBP images (FBP-1 and FBP-2) were calculated for each region. Paired Student *t* tests were performed to examine the difference between a subject's MRP and FBP images and across the myocardial regions. Therefore, the defined coefficients of variations were due to the reconstruction methods and not to variability in metabolism between subjects. $P < 0.05$ was considered to be statistically significant.

RESULTS

Visual quality of images reconstructed with the MRP and the FBP methods is shown in Figure 2. As can be seen, the MRP resulted in markedly enhanced image quality compared with the FBP. The radial artifacts, which are commonly seen outside of the object, are present only in the FBP images. Radioactivity concentrations of ventricles and myo-

TABLE 1
Correlation Coefficients (*r*) of rMBF, rOEF and $rMMRO_2$ Across Measures

	$r_{MRP\text{-}1 \text{ vs. } MRP\text{-}2}$	$r_{FBP\text{-}1 \text{ vs. } FBP\text{-}2}$
rMBF		
Lateral	0.895	0.819*
Anterior	0.886	0.797*
Septal	0.895	0.556†‖
rOEF		
Lateral	0.888	0.729‡
Anterior	0.923	0.828§
Septal	0.918	0.833§
$rMMRO_2$		
Lateral	0.930	0.870*
Anterior	0.951	0.844‡
Septal	0.944	0.746†‖

n = 108.

*$P < 0.05$, †$P < 0.0005$, ‡$P < 0.001$, §$P < 0.01$ vs. correlation between FBP-1 and FBP-2.

‖$P < 0.05$ vs. lateral and anterior regions.

rMBF = regional myocardial blood flow; rOEF = regional oxygen extraction fraction; $rMMRO_2$ = regional myocardial metabolic rate of oxygen consumption; MRP = median root prior; FBP = filtered backprojection.

cardium appeared more homogeneous in the MRP images. In addition, evident delineation of myocardial tissue boundaries with markedly sharper edges, especially in the septal region, are more clearly seen in the MRP images, compared with the FBP images.

Regional correlation coefficients of the parameters for the lateral, anterior and septal regions between MRP-1 and MRP-2 ($r_{MRP\text{-}1 \text{ versus } MRP\text{-}2}$), FBP-1 and FBP-2 ($r_{FBP\text{-}1 \text{ versus } FBP\text{-}2}$) are presented in Table 1. All the correlations were significantly higher when calculated from the MRP images than from the FBP images. The enhancement of regional correlation coefficients of rMBF and $rMMRO_2$ was most significant in the septal regions in the MRP images. The correlation coefficients of the parameters in the MRP images did not significantly differ across the myocardial regions.

Correlation plots of the values of rMBF, rOEF and $rMMRO_2$ for a total of 324 myocardial ROIs are shown in Figure 3. The correlation coefficients were significantly higher for rMBF, rOEF and $rMMRO_2$ derived from the MRP (MRP-1 versus MRP-2) than from the FBP (FBP-1 versus FBP-2) images.

Average values of rMBF, rOEF and $rMMRO_2$ calculated from the MRP and FBP images (MRP-1 and FBP-1) and their differences are shown in Table 2. The $rMMRO_2$ for all regions and rOEF for the anterior and septal regions were significantly higher when calculated from the MRP images than from the FBP images.

Variations of rMBF, rOEF and $rMMRO_2$ in the lateral, anterior and septal regions are presented in Table 3. The coefficients of variations of rMBF, rOEF and $rMMRO_2$ were significantly lower in all regions when calculated from the MRP images than from the FBP images. Independent of the

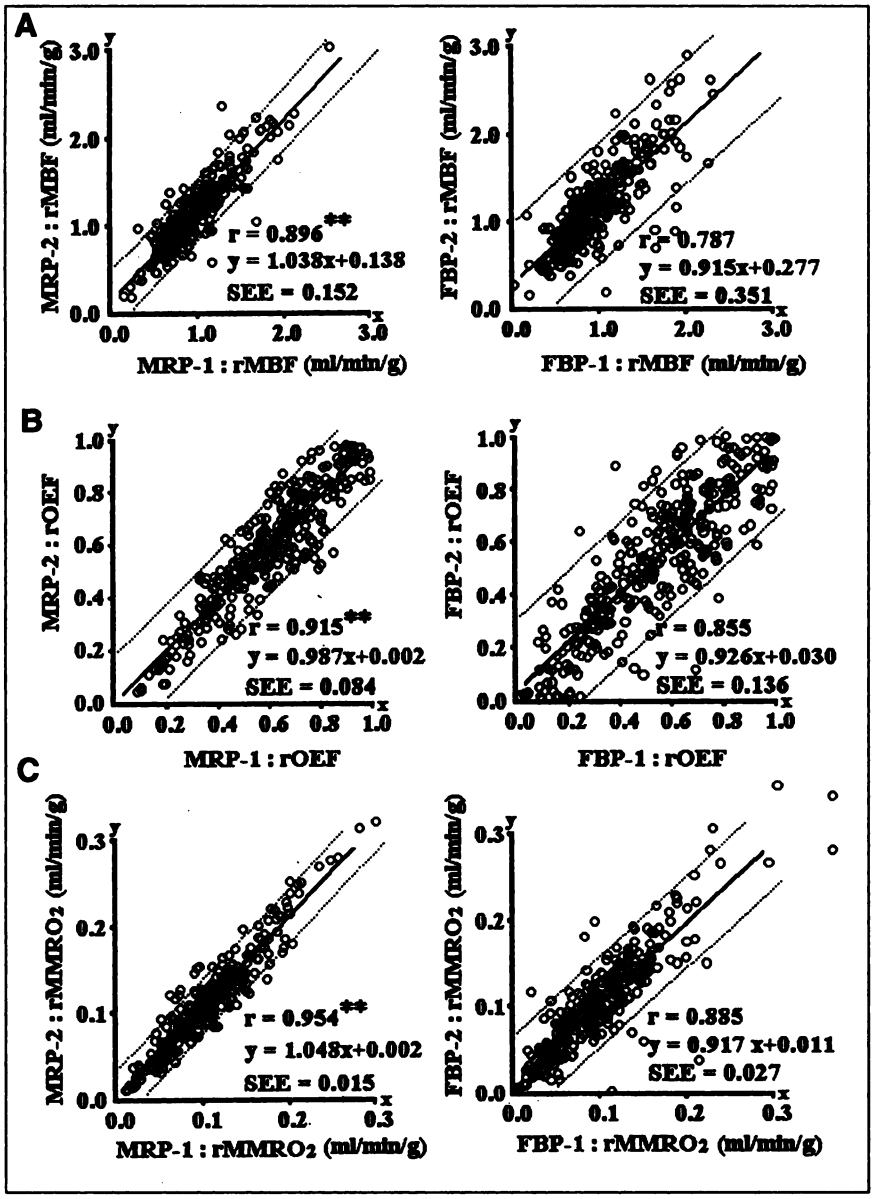

FIGURE 3. Plots of correlations between repeated measurements in MRP images (MRP-1 versus MRP-2) and in FBP images (FBP-1 versus FBP-2) for rMBF (A), rOEF (B) and $rMMRO_2$ (C) in 324 myocardial ROIs of 27 subjects. Regression lines and 95% confidence intervals are drawn. Correlations were significantly higher when calculated from MRP images (**$P < 0.001$) than from FBP images.

TABLE 2
Average Values, Differences and Correlations of rMBF, rOEF and $rMMRO_2$ Between MRP-1 and FBP-1

	MRP-1	FBP-1	Difference	Correlation coefficient
rMBF (mL/min/g)				
Lateral	0.940 ± 0.336	0.912 ± 0.395	0.027 ± 0.157	0.921
Anterior	1.066 ± 0.299	1.033 ± 0.302	0.033 ± 0.229	0.822
Septal	0.866 ± 0.372	0.866 ± 0.433	0.001 ± 0.342	0.648
rOEF				
Lateral	0.688 ± 0.148	0.668 ± 0.183	0.020 ± 0.117	0.769
Anterior	0.653 ± 0.180	0.595 ± 0.210	0.058 ± 0.126*	0.804
Septal	0.452 ± 0.208	0.380 ± 0.232	0.072 ± 0.167*	0.716
$rMMRO_2$ (mL/min/g)				
Lateral	0.116 ± 0.043	0.111 ± 0.047	0.006 ± 0.020†	0.897
Anterior	0.123 ± 0.047	0.117 ± 0.056	0.006 ± 0.032‡	0.832
Septal	0.072 ± 0.040	0.064 ± 0.043	0.009 ± 0.026*	0.803

n = 108.
*$P < 0.001$, †P 0.01 and ‡$P < 0.05$ between MRP-1 and FBP-1 by paired t test.
rMBF = regional myocardial blood flow; rOEF = regional oxygen extraction fraction; $rMMRO_2$ = regional myocardial metabolic rate of oxygen consumption; MRP = median root prior; FBP = filtered backprojection.

reconstruction method, the regional coefficient of variation of each parameter was significantly higher in the septal region ($P < 0.05$).

DISCUSSION

In this study, we compared reproducibility and variability of the myocardial parameters derived from the MRP images with those from the FBP images to examine the clinical advantage of the MRP reconstruction method. To improve the stability of quantitative measurements of the myocardial oxygen metabolism, we applied the MRP reconstruction method. $[^{15}O]CO$, $[^{15}O]H_2O$ and $[^{15}O]O_2$ were used as tracers, because the $rMMRO_2$ is calculated as a product of rMBF, rOEF and oxygen content in arterial blood.

TABLE 3
Coefficient of Variations of rMBF, rOEF and $rMMRO_2$ in MRP and FBP

	MRP	FBP
rMBF		
Lateral	21.3 ± 6.0	24.3 ± 6.8*
Anterior	20.5 ± 8.8	24.0 ± 9.4*
Septal	33.7 ± 14.8	42.1 ± 17.6*
Global	23.5 ± 11.3	30.1 ± 14.7†
rOEF		
Lateral	17.7 ± 7.0	20.9 ± 8.7†
Anterior	21.2 ± 10.0	27.1 ± 12.9†
Septal	28.6 ± 14.7	48.4 ± 23.2†
Global	21.0 ± 11.1	32.1 ± 19.8†
$rMMRO_2$		
Lateral	20.5 ± 7.2	22.6 ± 8.7*
Anterior	18.2 ± 10.8	23.7 ± 11.7*
Septal	35.4 ± 16.1	44.6 ± 24.4*
Global	23.1 ± 13.2	30.3 ± 19.1†

n = 27 (global: n = 81).
*$P < 0.05$ and †$P < 0.001$ between MRP and FBP by paired t test.
rMBF = regional myocardial blood flow; rOEF = regional oxygen extraction fraction; $rMMRO_2$ = regional myocardial metabolic rate of oxygen consumption; MRP = median root prior; FBP = filtered backprojection.

Images reconstructed with the MRP method had better visual quality than images reconstructed with the conventional FBP method (Fig. 2). Thus, the MRP images enable easier and more accurate definition of ROIs on the myocardial wall. This is of great importance, because accurate localization of ROIs on the myocardium and left ventricle is required for stable quantitative myocardial PET studies (*13*). In dynamic PET studies performed with ^{15}O-labeled tracers and short acquisition time, low myocardial tracer uptake or heterogeneous radioactivity might yield inaccurate measurements of myocardial parameters (*14*). The use of an iterative reconstruction algorithm has been suggested to be a feasible procedure for the problem (*15*). However, the previously applied iterative MLEM reconstruction methods have some disadvantages that might lead to errors in quantification of PET data. The MRP method applied in this study is insensitive to the number of iterations, and, thus, the iterative process can be continued long enough to achieve the quantitatively accurate value without increasing the noise in the images (*7*). This is opposite to the MLEM method, in which the iterations have to be stopped early enough to be able to obtain visually good results in the images. We have demonstrated the MRP method to be the most accurate reconstruction method at pixel level when compared with FBP and MLEM reconstruction methods (*7*).

In the present study, we found that the MRP reconstruction method improved the reproducibility of all calculated

parameters. The correlation coefficients between the two sets of rMBF, rOEF and $rMMRO_2$ calculated from the MRP images were significantly higher than those calculated from the FBP images (as shown in Table 1 and Fig. 3). The main reason for the better reproducibility of the MRP images is the reduced noise of the images, which leads to more homogeneous radioactivity in the myocardial wall.

In addition to the visual quality of the images and the reproducibility of the results, it is of great importance whether the use of a different reconstruction method changes the quantitative results of the PET measurements. Previously, Alenius and Ruotsalainen (*7*) have demonstrated quantitatively similar results from a large ROI in images reconstructed with the MRP, the FBP or the MLEM method. In this study, $rMMRO_2$ values calculated from the MRP images appeared to be higher in all regions when compared with the values calculated from the FBP images (Table 2). Also, rOEF values in the anterior and septal regions were significantly higher when derived from the MRP than from the FBP images. However, rMBF appeared to be insensitive to the reconstruction method.

The use of median filter in the MRP reconstruction algorithm preserves the edges of the myocardium precisely, and, consequently, the partial volume effect is reduced. In the FBP images, partial volume effect is known to result in an underestimation of the radioactivity concentration of the myocardium (*16*). Reduced partial volume effect of the MRP images is one explanation for the significantly higher rOEF and $rMMRO_2$ values. However, the partial volume effects should be appropriately corrected also with FBP images when ^{15}O water models, such as in this study, are applied (*8,9*). The most probable reason for better results is that the FBP method produces reconstruction artifacts, which vary between different time frames and, thus, increase the variations of the calculated metabolic parameters (*7*).

In this study, we found that the enhanced resolution of the MRP images improved reproducibility most in the anterior and septal regions, where partial volume effect and spillover from the right ventricle are most marked (*11*). Coefficients of variation of rMBF, rOEF and $rMMRO_2$ were significantly lower in all regions of the MRP images when compared with the variability of the same parameters calculated from the FBP images (Table 3).

The major limitation of the iterative reconstruction methods, including MRP, is that, even though ordered subsets are applied, considerable computing time is required compared with the standard FBP method. However, it is probable that in the near future computing time of the MRP method will be reduced with faster hardware and optimized software code.

CONCLUSION

The MRP method reduces reconstruction artifacts, preserves myocardial edges and homogeneity of radioactivity in the myocardial wall in comparison with the FBP method. In this study, we observed significantly higher reproducibility and lower variability in the metabolic parameters calculated from the MRP images than from the FBP images. The MRP reconstruction method improved accuracy and stability of clinical quantification of myocardial blood flow and oxygen metabolism with ^{15}O. Thus, we highly recommend application of the MRP reconstruction method in quantitative myocardial studies that use ^{15}O and PET.

REFERENCES

1. Strauss LG. Fluorine-18 deoxyglucose and false-positive results: a major problem in the diagnostics of oncological patients. *Eur J Nucl Med.* 1996;23:1409–1415.
2. Shepp LA, Vardi Y. Maximum likelihood reconstruction for emission tomography. *IEEE Trans Med Imaging.* 1982;1:113–121.
3. Herman GT, Odhner D. Performance evaluation of an iterative image reconstruction algorithm for positron emission tomography. *IEEE Trans Med Imaging.* 1991;10:336–346
4. Knesaurek K, Machac J, Vallabhajosula S, Buchsbaum MS. A new iterative reconstruction technique for attenuation correction in high-resolution positron emission tomography. *Eur J Nucl Med.* 1996;23:656–661.
5. Llacer J, Veklerov E, Baxter L, et al. Results of a clinical receiver operating characteristic study comparing backprojection and maximum likelihood estimator images in FDG PET studies. *J Nucl Med.* 1993;34:1198–1203.
6. Veklerov E, Llacer J. Stopping rule for the MLE algorithm based on statistical hypothesis testing. *IEEE Trans Med Imaging.* 1987;6:313–319.
7. Alenius S, Ruotsalainen U. Bayesian image reconstruction for emission tomography based on median root prior. *Eur J Nucl Med.* 1997;24:258–265.
8. Iida H, Rhodes CG, Araujo LI, et al. Noninvasive quantification of regional myocardial metabolic rate for oxygen by use of $^{15}O_2$ inhalation and positron emission tomography: theory, error analysis, and application in humans. *Circulation.* 1996;94:792–807.
9. Iida H, Rhodes CG, Silva R, et al. Myocardial tissue fraction—correlation for partial volume effects and measure of tissue viability. *J Nucl Med.* 1991;32:2169–2175.
10. Iida H, Takahashi A, Tamura Y, Ono Y, Lammertsma AA. Myocardial blood flow: comparison of oxygen-15-water bolus injection, slow infusion and oxygen-15-carbon dioxide slow inhalation. *J Nucl Med.* 1995;36:78–85.
11. Iida H, Rhodes CG, Silva R, et al. Use of the left ventricular time-activity curve as a noninvasive input function in dynamic oxygen-15 water positron emission tomography. *J Nucl Med.* 1992;33:1669–1677.
12. Iida H, Kanno I, Takahashi A, et al. Measurement of absolute myocardial blood flow with $H_2{}^{15}O$ and dynamic positron-emission tomography. Strategy for quantification in relation to the partial-volume effect. *Circulation.* 1988;78:104–115.
13. Milcinski M, Henze E, Lietzenmayer R, et al. Reproducibility of quantitative hexakis-2-methoxyisobutylisonitrile single photon emission tomography in stable coronary artery disease. *Eur J Nucl Med.* 1991;18:17–22.
14. Landoni C, Bettinardi V, Lucignani G, Gilardi MC, Striano G, Fazio F. A procedure for wall detection in [^{18}F]FDG positron emission tomography heart studies. *Eur J Nucl Med.* 1996;23:18–24.
15. Resnick SM, Karp JS, Turetsky B, Gur RE. Comparison of anatomically-defined versus physiologically based regional localization: effect on PET FDG quantitation. *J Nucl Med.* 1993;34:2201–2207.
16. Hutchins GD, Caraher JM, Raylman RR. A region of interest strategy for minimizing resolution distortions in quantitative myocardial PET studies. *J Nucl Med.* 1992;33:1243–1250.